A Whole Exome Sequencing Study of a small Indian Autosomal Dominant Polycystic Kidney Disease Patient Cohort

Chandra Devi[a], Shivendra Singh[b], Bhagyalaxmi Mohapatra[c], Ashok Kumar[d], Sanjay Vikrant[e], Rana Gopal Singh[f], Pradeep Kumar Rai[g], and Parimal Das[a],*

a. Centre for Genetic Disorders, Institute of Science, Banaras Hindu University, Varanasi, U.P., India-221005
b. Department of Nephrology, Institute of Medical Sciences, Banaras Hindu University, Varanasi, U.P., India-221005
c. Department of Zoology, Institute of Science, Banaras Hindu University, Varanasi, U.P., India-221005
d. Department of Pediatrics, Institute of Medical Sciences, Banaras Hindu University, Varanasi, U.P., India-221005
e. Department of Nephrology, AIIMS, Bilaspur, Himachal Pradesh, India-174001
f. Department of Medicine, Heritage Institute of Medical Science, Varanasi, U.P., India-221311
g. Nephrology Department, Opal Hospital , Kakarmatta , Varanasi, U.P., India- 221108

***Correspondence**: parimal@bhu.ac.in
Address- Centre for Genetic Disorders, Institute of Science, Banaras Hindu University, Varanasi, U.P., India-221005

Abstract

Autosomal Dominant Polycystic Kidney Disease is characterized by renal cyst development, often leading to kidney enlargement and failure. We conducted whole exome sequencing on 14 participants (12 families) from an Indian cohort. Our analysis revealed a spectrum of genetic variants, predominantly in the *PKD1*. These in *PKD1* included missense variants such as p.Glu2937Lys (c.8809G>A) and p.Gly2310Arg (c.6928G>A), p.Asp2095Gly (c.6284A>G), p.Thr938Met (c.2813C>T), p.Trp967Arg (c.2899T>C), p.Glu593* (c.1777G>T), frameshift variants p.Gln149fs*141 (c.445delC), p.Ser3305fs*84 (c.9914_9915delCT), p.His1347fs*83 (c.4041_4042delCA), and p.Leu2776fs*87(c.8327_8363delTGGCGGGCGAGGAGATCGTGGCCCAGGGCAAGCGCTC), intronic splice site variant c.8017-3C>G, nonsense variant p.Glu593* (c.1777G>T) and in *PKD2* missense variant p.Ser370Asn (c.1109G>A). While one individual carried intronic (c.2358+5G>A) and 3'UTR (c.*174G>T) variants in *PKD2* only another individual carried variants in both *PKD1* and *PKD2*, suggesting potential genetic complexity. Clinical data revealed diverse presentations. Age at diagnosis varied widely. Patients with frameshift variants exhibited earlier onset and severe manifestations, including bilateral ADPKD. One proband had right unilateral ADPKD. Involvement of liver, a common extra-renal manifestation, was also observed. Heterogeneity at phenotypic and at allelic level was observed in our cohort. In this study, using WES of a trio, a frameshift-truncation deletion [c.32del/p.Leu11ArgfsTer61] in *MIOX* was found to be associated with the disease shared by both the affected and early diagnosed mother and daughter carrying *PKD1* missense variant, which had not been previously reported in ADPKD. Further, differential gene expression analysis using data from GEO database showed reduced MIOX expression in ADPKD cystic samples compared to minimal cystic tissues and controls. MIOX is an enzyme specific to renal tubules and catalyses the initial step of the kidney-based myoinositol catabolism. Both affected candidates also shared benign variants and other variations of uncertain significance which may influence the disease development. Further functional analysis will clarify how MIOX contributes to the disease. The study limitations include the small sample size and the need for validation in larger cohorts. Our findings highlight the importance of genetic analysis in ADPKD management especially to facilitate personalized therapeutic strategies.

Keywords: ADPKD, Whole Exome Sequencing, *PKD1*, *PKD2*, MIOX, differential gene expression

Highlights:

- Identified variants in *PKD1* and *PKD2* through whole exome sequencing in ADPKD patients, affecting different protein regions.
- Variants include non-synonymous coding changes, frame-shift deletions, and splice site alterations.
- Clinical features and age at diagnosis varied widely, with common symptoms including flank pain, fatigue.
- Frameshift deletion in *MIOX*, associated in one PKD1 trio, implicates its role in ADPKD pathogenesis.
- DGE analysis of dataset from database reveals downregulation of MIOX in ADPKD tissue samples highlighting its role in potential molecular pathways in ADPKD progression.

Graphical abstract

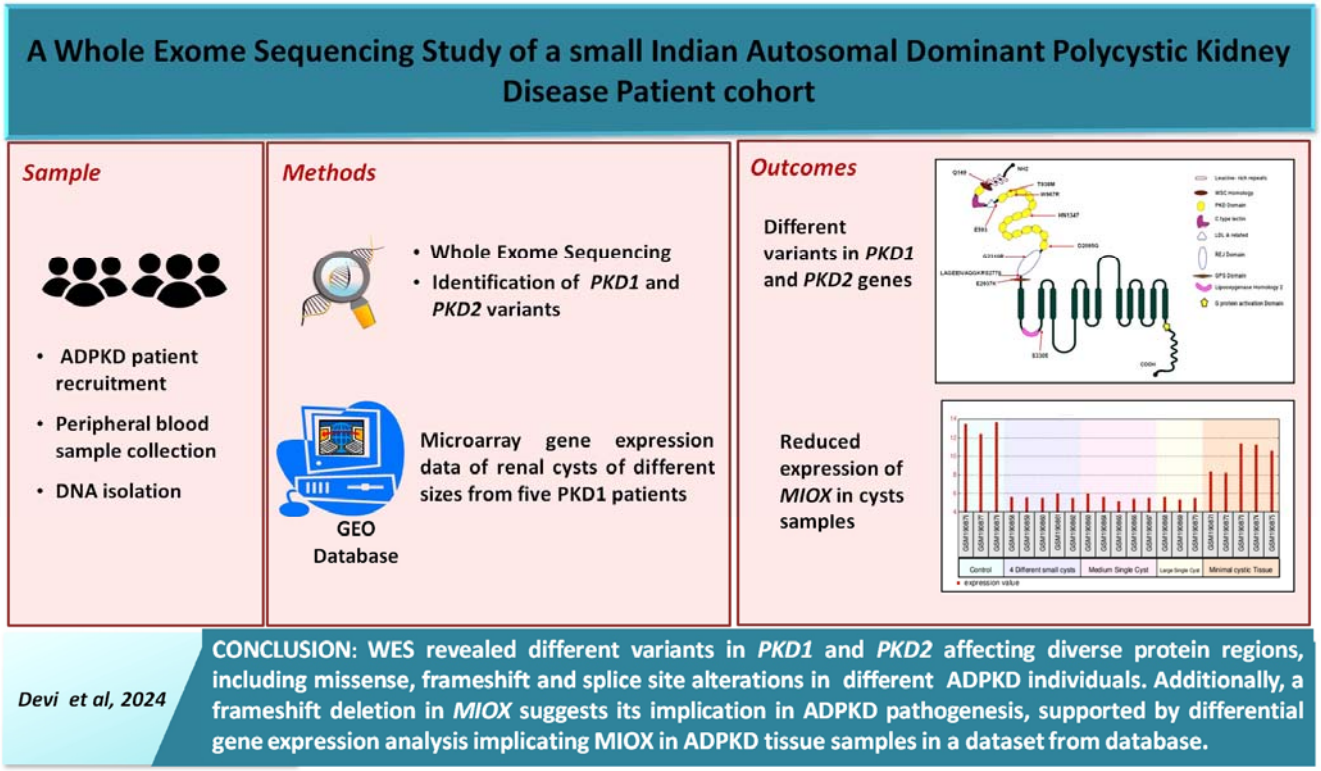

Introduction

Autosomal Dominant Polycystic Kidney Disease (ADPKD) is a common hereditary renal disorder affecting 1 in 500 - 1,000 individuals worldwide and is characterized by the development of multiple fluid-filled cysts in the kidneys, leading to progressive renal dysfunction [1, 2]. ADPKD is primarily caused by mutations in the *PKD1* (~75%) and *PKD2* (~15% -18%) which encode for polycystin-1 (PC1) and polycystin-2 (PC2) proteins, respectively and the remaining 7-10% of the cases remain genetically unresolved, and sporadic and mosaic ADPKD cases have also been observed [3–5]. This condition is genetically and phenotypically diverse, comprising a wide range of signs and severity levels even within the same family [6]. The prevalence of PKD also varies among different ethnic groups. Key features include renal cysts leading to kidney enlargement and failure, in many cases liver cysts causing hepatomegaly, and intracranial aneurysms, posing a risk of hemorrhagic stroke. In addition to these cardinal manifestations, ADPKD can also present with various extra renal manifestations and complications such as hypertension, urinary tract infections, renal stones, hematuria, proteinuria, renal insufficiency, and chronic pain. ADPKD has also been associated with an increased risk of cardiovascular abnormalities, such as left ventricular hypertrophy and valvular abnormalities, as well as abnormalities in other organs, including the pancreas, spleen, and reproductive system [7].

The diagnosis of ADPKD involves clinical evaluation and various imaging techniques, including ultrasonography, CT scans and MRI to detect renal cysts and assess their size and number [8, 9]. Genetic testing is essential, especially in cases with atypical presentations or uncertain diagnoses, to confirm pathogenic variations in the *PKD1* or *PKD2* genes and differentiate ADPKD from other kidney diseases. *PKD1* is a large gene that spans a 52kb region of genomic DNA and presents a challenge for direct PCR and Sanger sequencing for mutation analysis due to the presence of six pseudogenes [10]. Adding to the genetic complexity of the disease, recent studies have identified *GANAB*, *DNAJB11*, *ALG9*, *IFT140* as minor/associated genes [3, 5, 11]. Next-Generation Sequencing (NGS), such as Whole Exome Sequencing (WES), offers a comprehensive approach to analyzing genetic profiles, aiding in better understanding and management of PKD [12, 13]. The considerable genetic heterogeneity observed in *PKD1*

variants contributes to diverse clinical presentations and disease progression among affected individuals [5, 11]. While some variants result in severe disease manifestations early in life, others exhibit a more indolent course with later onset of symptoms [14, 15]. While extensive genetic analyses have been conducted on ADPKD cohorts globally, there remains a need for further exploration, particularly in diverse populations such as the Indian population, to elucidate the full spectrum of genetic variations contributing to the disease. Accurate classification, treatment, and monitoring of the disease rely on the detection of pathogenic variants in candidate genes such as *PKD1* and *PKD2*.

In our study, we used WES to identify pathogenic variants related to ADPKD major candidate genes highlighting the importance of molecular genetics in diagnosing and managing the disease. Also, using WES of a trio, a frameshift-truncation deletion [c.32del/p.Leu11ArgfsTer61] in *MIOX* was found to be associated with the disease shared by both the early diagnosed affected mother and daughter carrying *PKD1* missense variant, which has not been previously reported in ADPKD or other polycystic kidney diseases. In addition, the differential gene expression analysis the cystic tissue samples (GEO dataset: GSE7869) revealed a remarkable reduction in *MIOX* gene expression. *MIOX* encodes Myo-Inositol Oxygenase, which expresses exclusively in renal tubules and catalyzes the first step of myoinositol catabolism pathway predominantly occurring in the kidney [16]. While further functional evaluation is needed to elucidate the precise role of this variation in disease progression, the study highlights the potential of WES as a tool for PKD diagnosis and towards enhancing the scope for practicing personalized medicine.

Material and methods

Sample collection and DNA isolation

The 14 participants (from 12 families) were recruited from Sir Sunderlal Hospital, Banaras Hindu University, with informed consent obtained from all participants. Each sample was assigned a unique study code to ensure confidentiality and anonymity throughout the research process. The study received approval from the Institute Ethical Committee of the Institute of Science, Banaras Hindu University. Genomic DNA was extracted from peripheral blood samples using the standardized salting-out method [17]. Assessment of DNA quality and quantity was performed using spectrophotometric analysis (Nanodrop 2000, Thermo Scientific Inc.) or

fluorometry-based methods (DNA Assay BR, Invitrogen, Cat# Q32853 / Qubit High Sensitivity Assay, Invitrogen).

Whole Exome Sequencing

WES was performed using Illumina Next-Generation Sequencing. The WES platform targeted approximately 30Mb of the human exome, covering around 99% of the regions in CCDS and RefSeq. The mean sequencing depth was 80-100X, with more than 90% coverage of the target regions at a depth of 20X. Duplicate reads were removed, and base quality was recalibrated to ensure high-quality data. The reads were aligned to the human reference genome GRCh37 (hg19). Variant identification followed the GATK best practice framework, and variants were annotated using databases such as OMIM, GWAS, GNOMAD, and 1000Genome. The annotated variants underwent filtration based on several criteria including gnomAD genome allele frequency of ≤ 0.01 or NA (not available), read depth of ≥ 20, pathogenicity, and functional impact.

Gene Expression Data Source for Differential Gene Expression Analysis

The GEO database, GSE7869, from which the microarray gene expression data from renal cysts of different sizes of five PKD1 patients was retrieved, includes small cysts (<1 ml, n = 5), medium cysts (10–20 ml, n = 5), large cysts (>50 ml, n = 3), minimally cystic tissue (MCT, n = 5), and non-cancerous renal cortical tissue from three nephrectomized kidneys with isolated renal cell carcinoma as normal control (n = 3). The samples were examined using the Human Genome U133 Plus 2.0 Array chip platform from Affymetrix.

Differential Gene Expression Analysis

The raw data were normalized using the using R - RMA normalization followed by BiocManager::install (version = "3.12") BiocManager::install ("GEOquery") BiocManager::install ("affy") BiocManager::install ("hgu133a.db", type = "source") BiocManager::install ("hgu133acdf") Calling Libraries: library (GEOquery) library (affy) library (hgu133a.db) library (hgu133acdf). The limma function package of the R language (version 3.5.2) was used for the differentially expressed gene analysis [18], and the absolute logarithmic

conversion of the differential expression multiple (Log2FC) value >2 and FDR 0.05 were used as screening criteria.

Results

Clinical Features

Our study involved WES of 14 participants (12 probands, 1 affected relative, and 1 normal) from the Indian population, revealing different variants within the *PKD1* and *PKD2* genes. Both male and female patients were included, with ages ranging from 20 to 56 years at the time of sampling. The clinical profiles of the ADPKD patients in our cohort exhibited a spectrum of manifestations characteristic of the disease. A significant proportion of patients reported a positive family history of ADPKD, consistent with the autosomal dominant inheritance pattern of the disease. The enlarged kidney size with multiple cysts and bilateral involvement was predominant among the patients. Only one proband (individual with given ID 10_CD103) presented with unilateral kidney cysts and the sibling of this proband also exhibited unilateral kidney cysts at the teenage. Liver cysts were also noted in three cases. Patients reported a range of systemic symptoms such as flank pain, weakness, fatigue, and hematuria associated with ADPKD. These included flank pain which was a common complaint among the cohort, often attributed to cyst enlargement or hemorrhage within the kidneys. Generalized weakness and fatigue were also prevalent, reflecting the systemic impact of chronic kidney disease on overall health and vitality.

PKD1 Variants

By applying a stringent filter based on gnomAD genome allele frequency of ≤ 0.01 or NA (not available), we observed that the majority of ADPKD individuals (11 out of 12 probands) exhibited heterozygous variants in *PKD1* except one carrying a homozygous missense variant, signifying its predominant role in ADPKD pathogenesis in our cohort. Among these, two individuals carried the same variant in the intronic splice site region of the *PKD1* gene, while another individual carried variants in both *PKD1* and *PKD2*. One individual was found to carry a

variant in the *PKD2* gene. Different variants (Table 2) in different ADPKD individuals were identified in the *PKD1* gene viz. missense variants p.Glu2937Lys (c.8809G>A) in exon 24, p.Gly2310Arg (c.6928G>A) in exon 16, synonymous variant p.Thr2710= (c.8130C>T) in exon 22, Intronic-Splice Site Region variant c.8017-3C>G in exon 21 in two individuals, nonsense variant c.1777G>T (p.Glu593*) in exon 9, frameshift variants: p.Gln149fs*141 (c.445delC) in exon 4, p.Ser3305fs*84 (c.9914_9915delCT) in exon 29, p.His1347fs*83 (c.4041_4042delCA) in exon 15, novel Codon Deletion p.Ser2792_Leu2793del (c.8374_8379delAGCCTG) in exon 23, novel p.Asp2789_Pro2790delinsGlu (c.8367_8369delCCC) Codon Change plus Codon Deletion in exon 23, novel p.Leu2776fs*87 (c.8327_8363delTGGCGGGCGAGGAGATCGTGGCCCAGGGCAAGCGCTC) Frameshift

in exon 23. The frameshift variants p.Gln149fs141, p.Ser3305fs84, and p.His1347fs*83 were classified as pathogenic variants according to ACMG criteria and were not reported in population databases (Table 3).

The exons and corresponding amino acid intervals are mentioned in table 4. The amino acid number and corresponding motif/domains are mentioned in table 5 and 6, the variants affecting the domain in protein structure are depicted in figure 1 and the anticipated functions of each domain in table7.

***PKD2* Gene Variants**

The variants identified in the *PKD2* gene are Intronic, Splice Site Region c.2358+5G>A in Exon 12, c.*174G>T in 3' UTR (Untranslated Region), Missense p.Ser370Asn (c.1109G>A) variant in Exon 5 (Table 2). The variants c.2358+5G>A and c.*174G>T with ACMG classifications and predicted to be deleterious and benign, respectively. These variants were reported in population databases and were categorized as uncertain significance in ClinVar.

Predictions and Availability in Databases

Predictions of pathogenicity were based on ACMG criteria, MUT Assessor scores, and various computational tools (Table 3). Variants were cross-referenced with population databases such as Gnomad genome, ExAC and 1000G, as well as ClinVar, to assess their prevalence and significance. Some variants were not found in population databases and had limited evidence in literature or ClinVar (Table 3).

WES of a Trio

MIOX was filtered out to have the frameshift-truncation deletion [c.32del/p.Leu11ArgfsTer61] shared by both affected mother and daughter carrying *PKD1* c.2899T>C, p.Trp967Arg missense variant. The heterozygous deletion variant of the *MIOX* was identified as the top possible disease associated variant. This variant was cross-validated bi-directionally by Sanger sequencing (figure 2A). The frameshift deletion leads to truncated protein of 70 amino acids as compared to wild protein of 285 amino acids. The alignment of 285aa long normal and 70aa long mutated MIOX protein sequence is shown in figure 2B. As per the information available on the databases (Proteomics DB and MOPED) the MIOX protein specifically expresses in the kidney (figure 3C).

Differential Gene Expression Analysis

The normalized gene expression data of the cysts is shown in figure 4A. The analysis revealed that the cyst samples assembled together as a distinct group, while the minimal cystic tissues and normal renal cortical samples sorted together as a separate group (figure 4B). This indicates the similarity in the gene expression pattern between renal cysts of varying sizes, as well as between minimal cystic tissues and normal renal cortical tissue. In addition, the expression profile analysis of *MIOX* reveal that its expression level is reduced in cystic samples compared to minimal cystic tissues and control tissue samples, suggesting a potential role of this gene in the development of polycystic kidney disease.

Discussion

ADPKD is a genetic disorder characterized by progressive cyst formation and enlargement of the kidneys, often leading to end-stage kidney disease. The genetic basis of ADPKD is heterogeneous, with PKD1 (~75% of cases) and PKD2 (~15% of cases) being the most common loci, and *GANAB, DNAJB11, ALG9,*and *IFT140* being minor genes [4, 5, 19]. PKD is a ciliopathy, a disease associated with defects in the function of primary cilia, and many syndromic ciliopathies exhibit a PKD phenotype [20]. *PKD1* pathogenic variants are associated with ADPKD, which manifests as renal and liver cysts, intracranial aneurysms, pain, nephrolithiasis,

and end-stage renal disease. Understanding the genetic basis of ADPKD is crucial to understand its pathogenesis, identifying potential therapeutic targets, and improving clinical management strategies. Improving outcome, preventing complications, and initiating effective treatment rely heavily on accurate diagnosis. Molecular diagnosis also plays a critical role in the management of the diseases. WES is now becoming the choice of quick and accurate diagnosis for PKD and practicing personalized medicine. Given the complexity of the disease genetic testing in combination with clinical phenotypes offers definitive diagnosis contributing to better prognosis, clinical care, diagnosis in atypical cases, and family planning [12, 13, 21].

In this study, we conducted WES on a small cohort of 14 participants (from 12 families). Familial ADPKD was reported in all cases but one, indicating a clear hereditary pattern consistent with the autosomal dominant inheritance of the disease supporting the genetic basis of ADPKD. The imaging studies revealed multiple cysts of varying sizes in the kidneys. While bilateral involvement was predominant among the patients, one proband (individual coded 10_CD103) presented with unilateral kidney cysts, an uncommon finding in ADPKD [22]. Intriguingly, the sibling of this proband also exhibited unilateral kidney cysts at the teenage. ADPKD is typically known for bilateral involvement of the kidneys. This case may align with the unilateral renal cystic disease (URCD) which can be a manifestation of early-stage ADPKD particularly in pediatric cases [23]. In this case of unilateral ADPKD, the initial unilateral involvement emphasizes the need for careful diagnosis and regular long-term monitoring, as the disease may progress to asymmetric bilateral involvement over time. This supports the importance of considering ADPKD even in such cases ensuring appropriate management and follow-up. Liver cysts were noted in three cases. Patients reported a range of systemic symptoms associated with ADPKD. These included flank pain, which was a common complaint among the cohort, often attributed to cyst enlargement or hemorrhage within the kidneys. Generalized weakness, fatigue, kidney stone, appetite changes, nausea, anemia, hematuria, and other non-specific symptoms (Table 1) in the cohort reflect the systemic impact of the disease on overall health and vitality. Despite the presence of common features, the cohort displayed clinical heterogeneity in terms of age at presentation, symptomatology, and disease severity. This highlights the heterogeneity of ADPKD and the variability in disease presentation among affected individuals.

Analysis of the WES data identified several genetic variants within the *PKD1* and *PKD2* which are known to be major candidate genes of ADPKD. The variants in *PKD1* were more prevalent in our cohort, consistent with previous reports highlighting the predominant role of *PKD1* variants in ADPKD pathogenesis [17, 24]. Variants identified in *PKD1* included missense changes, nonsense variant, frameshift variants, and intronic splice site variants, each with varying degrees of pathogenicity as classified in ClinVar. The *PKD2* variants were also detected, albeit less frequently, emphasizing the contribution of both genes to ADPKD.

The variants identified span various regions of the *PKD1* and *PKD2*, potentially impacting protein structure and function. The table 1, 2 and 3 presents clinical and genetic information of patients with ADPKD, detailing the approximate age at diagnosis, gene, variant, effect of variant, exon number, and protein region affected and predictions using various tools. Individual 6_CD66 harbored a frameshift variant in the exon 29 of the *PKD1* gene (p.Ser3305fs*84, c.9914_9915delCT) which is present in between the LH2 and PKD cation channel region of PC1 protein. This patient, diagnosed at age early 50s, presented with bilateral ADPKD, characterized by multiple cysts and calculi in both kidneys (Table 1-3). Clinical symptoms included flank pain and blood in urine, indicating more severe disease manifestations. Another frameshift mutation was observed in individual 7_CD73, with a variant in *PKD1* exon 15 leading to a premature stop codon (p.His1347fs*83, c.4041_4042delCA). This will lead to a truncated protein upto PKD 7th domain. This patient diagnosed at late teenage, exhibited bilateral ADPKD and reported symptoms of flank pain, indicating early-onset. Both patients' kidney sizes were larger than average, indicating a more advanced stage of the disease. Individual 8_CD78 (ADPKD with hepatomegaly), also diagnosed at late teenage, exhibited frameshift deletion in the exon 23 of *PKD1* gene impacting in REJ domain profile region. The presence of a frameshift variant in exon 15 and a larger deletion in exon 23 may have contributed to the early onset and severity of the disease phenotype. Individual 4_CD25 harbored a frameshift variant p.Gln149fs*141, c.445delC in *PKD1* exon 4 causing a frameshift and deletion in the region between the LRR1 and WSC domain. This patient diagnosed at early 40s, had bilateral ADPKD with rare occurrences of symptoms such as flank pain and blood in urine.

A heterozygous nonsense variant, c.1777G>T (p.Glu593*), in exon 9 of *PKD1* was identified in 11_CD99 diagnosed at early 30s. This variant introduces a premature stop codon, resulting in a

truncated protein. The variant was absent in population databases, including gnomAD exomes and genomes however reported in publication (table 3).

Patient number 1_CD1 carried a missense variant in exon 24 of the *PKD1* gene (p.Glu2937Lys, c.8809G>A), classified as of uncertain significance, leading to a non-synonymous coding change in the REJ domain profile region, possibly affecting protein folding and function. This patient, diagnosed at mid 40s, presented with bilateral ADPKD, with a reported family history of the disease. Notably another patient 9_CD98, late 20s, exhibited grossly enlarged kidneys carried homozygous missense variant c.6928G>A (p.Gly2310Arg) in the *PKD1*, affecting the REJ Domain of PC1. Homozygosity for missense *PKD1*, as seen in this case, may contribute to the manifestation of early ADPKD, possibly through mechanisms involving gene dosage. Reports of homozygous mutations in *PKD1* and biallelic inheritance of missense variants highlight the role of gene dosage in determining disease severity [14, 25].

Patient 5_CD42 (diagnosed at late 20s) and patient 3_CD8 (diagnosed at late teenage) both carried intronic splice site variants in exon 21 of the *PKD1* gene (c.8017-3C>G) and exhibited bilateral ADPKD with multiple anechoic cysts. Patient 2_CD3, diagnosed at early 50s, experienced generalized body weakness, had synonymous and intronic variants in the *PKD2* gene, with reported bilateral ADPKD and multiple cortical and medullary cysts. The older age at diagnosis may suggest a slower disease progression and milder clinical phenotype, despite the presence of potentially pathogenic variants.

Liver cysts are a common extra-renal manifestation observed in patients with ADPKD. In our cohort, liver cysts were detected in three patients, notably in individual 8_CD78, who presented with multiple cysts in both kidneys, liver along with liver enlargement and simple cysts in right ovary. This patient exhibited symptoms of stomach ache, indicating potential compression effects of liver and kidney cysts. The presence of liver cysts in ADPKD patients can vary widely in terms of size, number, and associated symptoms [26]. While some patients may remain asymptomatic, others may experience discomfort or complications due to cyst growth and compression of adjacent structures.

The discrepancy in age at diagnosis between missense changes (diagnosis at mid 40s) and frameshift/nonsense change (diagnosis at late teenage and late 20s, respectively) within or near

the REJ domain region suggests a potential correlation between mutation type and disease onset timing in ADPKD. The frameshift mutations in *PKD1* have been associated with more severe clinical presentations, including bilateral involvement and symptomatic flank pain. In contrast, patients with synonymous and missense variants tended to have milder disease manifestations with fewer reported symptoms [17, 24, 27, 28]. The variants identified in the *PKD1* affect various protein regions, each with its potential impact on the function of PC1 (Table 7). For instance, the non-synonymous and frameshift deletion variants in or near the REJ domain profile region possibly disrupt the signal transduction, which is crucial for cell-cell interactions and signal transduction through PC-1. The frameshift or non-synonymous variant in the the 3rd, 7th, 16th PKD repeats may influence cellular processes mediated by these domains. Similarly, the frameshift variant between LRR1 and the WSC domain, the nonsense variant between the Lectin C-type domain and PKD 2nd repeat could disrupt critical interactions involved in cell signaling and renal development [29]. The presence of the same intronic splice site variation in the *PKD1* gene was observed in two individuals within our cohort. Functional studies such as RNA sequencing or splice assays may provide insights into the impact of this intronic variation on *PKD1* mRNA splicing and its association with ADPKD pathogenesis. The identification of individuals carrying variations in both the *PKD1* and *PKD2* raises questions about potential synergistic effects or genetic modifiers influencing disease severity and progression as the patient is diagnosed at an early age (late-teenage). The exon number and affected domains appear to influence disease severity and diverse clinical phenotypes in ADPKD patients. However, further larger studies are needed to elucidate the specific functional consequences of variants in different exons and their impact on disease progression in ADPKD.

In the other part of this study using WES of a trio (12_CD24 proband, CD24.1 proband's husband, CD24.2 affected daughter) identified a missense *PKD1* variant shared by both affected mother and daughter. Interestingly, a heterozygous frameshift deletion [c.32del/p.Leu11ArgfsTer61, Exon 2] in *MIOX*, subsequently validated by Sanger sequencing, was also shared by both the affected persons. The variant was screened using the dominant inheritance pattern. This deletion has not been previously reported as an ADPKD related variation. The frameshift deletion leads to a truncated protein of 70 amino acids as compared to the wild protein of 285 amino acids which disrupts the binding site according to primary structure prediction. *MIOX* encodes for a 32Kda myo-inositol oxygenase (MIOX), which is a

cytosolic enzyme expressed specifically in the renal proximal tubules, and is the first rate-limiting enzyme of myo-inositol catabolism. This enzyme is found to be upregulated in hyperglycemic conditions. MIOX is a single-domain protein with a mostly helical fold distantly related to the diverse HD domain superfamily. So far, studies have shown that MIOX plays a critical role in the metabolism of inositol, a carbohydrate molecule, and is involved in the regulation of glucose metabolism, insulin signaling, and oxidative stress response [16]. Studies have suggested the role of *MIOX* in insulin signaling in the renal proximal tubule cells and may play a role in the development of diabetic kidney disease [30]. Additionally, MIOX has been found to be involved in the regulation of oxidative stress, which can contribute to kidney injury in various disease states. *MIOX* promoter contains several response elements: oxidant-, antioxidant-, osmotic-, carbohydrate-, sterol-, response elements [30]. While the role of *MIOX* has been linked to acute kidney injury, tubulointerstitial renal fibrosis, diabetic-associated nephropathies, and reactive oxygen species (ROS) generation (figure 3A) [16, 31, 32], its role in ADPKD has not yet been reported. Recently, higher expression of *MIOX* has been reported in prostate adenocarcinoma [33].

As for *MIOX*, previous studies have explored the effects of overexpression and knockdown of *MIOX* in diabetic conditions. The current study identified a heterozygous frame shift deletion. This deletion leads to a premature termination of the MIOX protein, resulting in a truncated protein (70aa) that is much shorter than the wild-type MIOX protein (285aa). One possible impact of this deletion could be haploinsufficiency, where a single functional copy of the gene is insufficient to produce the required amount of functional protein necessary for normal cellular processes. This may lead to a reduction in the amount of functional MIOX protein below a threshold level, which could potentially trigger cyst formation. The other possibility could be a dominant-negative effect where the truncated protein created by heterozygous deletion may interfere with the function of the normal protein. This can disrupt the activity of protein complexes or signaling pathways, leading to disease.

The identification of a heterozygous frame-shift deletion in *MIOX* implies that this gene, along with the *PKD1* missense variant, may play a role in the early development of ADPKD in this specific trio, indicating a double heterozygous condition. The association of MIOX is further supported by the gene expression profile analysis of the data of cysts of variable sizes from GEO

database, which shows that the expression level of *MIOX* gene is reduced remarkably in cystic samples compared to minimal cystic tissues (MCT) and control tissue samples (figure 4E). These results indicate that the down-regulation of *MIOX* expression may play a significant role in the development of PKD. In addition to this, the down regulation of Klotho (KL) protein in the reference study done by Song X et al. in 2009 [34] is noteworthy, as its direct STRING interaction with MIOX can be seen in our STRING interaction network (figure 3B & 4F). The *KL* encoded protein is a type-I membrane protein which is related to beta-glucosidases. Decreased expression of this KL protein has been reported in individuals with chronic renal failure. This suggests that the down-regulation of KL protein may be linked to the reduced expression of *MIOX* and further investigation into the relationship between these genes may shed light on their role in PKD pathogenesis. Overall, these findings highlight the importance of understanding the complex interplay between various genes and their expression profiles in the development and progression of PKD.

The all variants but one indentified in our cohort were different from those previously reported in our laboratory's work [17]. The absence of identified variants in population databases and their submission in ClinVar without corresponding population frequency data highlight the need for population-specific genetic studies to fully capture the spectrum of disease-causing variants, particularly in understudied populations such as the Indian cohort in our study. Further functional studies, larger cohort analyses, and genotype-phenotype correlation studies would validate the pathogenicity of these variants and elucidate their impact on disease progression and clinical outcomes. The diversity of the variants suggests the genetic heterogeneity inherent in ADPKD, which may contribute to variability in disease presentation and progression among affected individuals. Understanding the genetic basis of ADPKD is crucial for improving diagnosis, prognosis, and the targeted therapies aimed at specific genetic mutations or pathways implicated in ADPKD pathogenesis which may benefit from the identification and characterization of novel variations, particularly those with potential functional significance.

Study Limitations and future directions

The small sample size of our study cohort limits the generalizability of the findings to larger populations. Future studies with larger cohorts are needed to validate the significance of

identified variations and elucidate their broader implications. Longitudinal studies incorporating clinical data and patient outcomes would establish genotype-phenotype correlations and assessing the prognostic value of identified variations in ADPKD progression.

Conclusion

Our WES study expands the repertoire of genetic variations associated with ADPKD in the Indian population, providing insights into the genetic heterogeneity and complexity of this disease. Further, this study also identifies a frame-shift deletion [c.32del/p.Leu11ArgfsTer61] in *MIOX* besides *PKD1* missense variant, shared by both affected individuals in a trio which is not earlier reported in ADPKD. The frame-shift deletion results in a truncated protein with only 70 amino acids, which disrupts the binding site according to primary structure prediction. The differential gene expression analysis also showed reduced expression of *MIOX* in cysts samples. Further functional investigation is needed to determine the involvement of the *MIOX* variation in disease progression. The identification of this mutation in *MIOX* in an ADPKD trio study provides a potential avenue for further exploratory studies into the genetic underpinnings of ADPKD. These findings highlight the importance of understanding the complex interplay between various genes and their expression profiles in the development and progression of PKD. Further research at a larger scale is needed to elucidate the functional significance of identified variants, their contribution to disease pathogenesis, and their potential implications for clinical management and genetic counseling in ADPKD patients.

Acknowledgements

We acknowledge the funding support provided by the Department of Biotechnology (DBT) and the Senior Research Fellowship to first author obtained from the Indian Council of Medical Research (ICMR), India. We acknowledge Mr. Prashant Ranjan, ICMR-SRF, Centre for Genetic Disorders, Institute of Science, Banaras Hindu University, for his contribution in Differential Gene Expression analysis done in this study. We also extend our appreciation to the participants for their invaluable contribution to this study.

Disclosure

The authors declare no conflict of interest.

References:

1. Nobakht N, Hanna RM, Al-Baghdadi M, et al (2020) Advances in autosomal dominant polycystic kidney disease: a clinical review. Kidney Med 2:196–208

2. Torres VE, Bennett WM Autosomal dominant polycystic kidney disease (ADPKD) in adults: Epidemiology, clinical presentation, and diagnosis. Uptodate Waltham, MA Uptodate Inc http//www uptodate com (Accesed December 27, 2019)

3. Cornec-Le Gall E, Torres VE, Harris PC (2018) Genetic complexity of autosomal dominant polycystic kidney and liver diseases. J Am Soc Nephrol 29:13–23

4. Hopp K, Cornec-Le Gall E, Senum SR, et al (2020) Detection and characterization of mosaicism in autosomal dominant polycystic kidney disease. Kidney Int 97:370–382

5. Lanktree MB, Haghighi A, di Bari I, et al (2021) Insights into autosomal dominant polycystic kidney disease from genetic studies. Clin J Am Soc Nephrol 16:790–799

6. Lanktree MB, Guiard E, Li W, et al (2019) Intrafamilial variability of ADPKD. Kidney Int Reports 4:995–1003

7. Nishio S, Tsuchiya K, Nakatani S, et al (2021) A digest from evidence-based clinical practice guideline for polycystic kidney disease 2020. Clin Exp Nephrol 25:1292–1302

8. Mallawaarachchi AC, Lundie B, Hort Y, et al (2021) Genomic diagnostics in polycystic kidney disease: an assessment of real-world use of whole-genome sequencing. Eur J Hum Genet 29:760–770

9. Pei Y, Hwang Y-H, Conklin J, et al (2015) Imaging-based diagnosis of autosomal dominant polycystic kidney disease. J Am Soc Nephrol 26:746–753

10. Harris PC, Ward CJ, Peral B, Hughes J (1995) Polycystic kidney disease. 1: Identification and analysis of the primary defect. J Am Soc Nephrol 6:1125–1133

11. Cornec-Le Gall E, Olson RJ, Besse W, et al (2018) Monoallelic mutations to DNAJB11 cause atypical autosomal-dominant polycystic kidney disease. Am J Hum Genet 102:832–844

12. Du N, Dong D, Sun L, et al (2021) Identification of ACOT13 and PTGER2 as novel candidate genes of autosomal dominant polycystic kidney disease through whole exome sequencing. Eur J Med Res 26:1–8

13. Zacchia M, Blanco FDV, Trepiccione F, et al (2021) Nephroplex: a kidney-focused NGS panel highlights the challenges of PKD1 sequencing and identifies a founder BBS4 mutation. J Nephrol 34:1855–1874

14. Bergmann C, von Bothmer J, Brüchle NO, et al (2011) Mutations in multiple PKD genes may explain early and severe polycystic kidney disease. J Am Soc Nephrol JASN 22:2047

15. Burgmaier K, Kilian S, Bammens B, et al (2019) Clinical courses and complications of young adults with autosomal recessive polycystic kidney disease (ARPKD). Sci Rep 9:7919

16. Deng F, Sharma I, Dai Y, et al (2019) Myo-inositol oxygenase expression profile modulates pathogenic ferroptosis in the renal proximal tubule. J Clin Invest 129:5033–5049

17. Raj S, Singh RG, Das P (2020) Mutational screening of PKD1 and PKD2 in Indian ADPKD patients identified 95 genetic variants. Mutat Res Mol Mech Mutagen 821:111718

18. Ritchie ME, Phipson B, Wu DI, et al (2015) limma powers differential expression analyses for RNA-sequencing and microarray studies. Nucleic Acids Res 43:e47–e47

19. Senum SR, Li YSM, Benson KA, et al (2022) Monoallelic IFT140 pathogenic variants are an important cause of the autosomal dominant polycystic kidney-spectrum phenotype. Am J Hum Genet 109:136–156

20. McConnachie DJ, Stow JL, Mallett AJ (2021) Ciliopathies and the kidney: a review. Am J Kidney Dis 77:410–419

21. Odland D (2021) A patient perspective on genetic testing for ADPKD: the lack of complete genetic information, especially early in the course of the disease, is harming adult autosomal dominant polycystic kidney disease (ADPKD) patients. Clin. J. Am. Soc. Nephrol. 16:671–673

22. Shin C, Berliner L (2021) Case report: Atypical polycystic kidney disease. Radiol Case Reports 16:1643–1645

23. Gulzar M, Bakhsh M, Yonis H, et al Unilateral Renal Cystic Disease (URCD)

24. Pandita S, Ramachandran V, Balakrishnan P, et al (2019) Identification of PKD1 and PKD2 gene variants in a cohort of 125 Asian Indian patients of ADPKD. J Hum Genet 64:409–419

25. Audrézet M-P, Corbiere C, Lebbah S, et al (2016) Comprehensive PKD1 and PKD2 mutation analysis in prenatal autosomal dominant polycystic kidney disease. J Am Soc Nephrol 27:722–729

26. Kataoka H, Watanabe S, Sato M, et al (2021) Predicting liver cyst severity by mutations in patients with autosomal-dominant polycystic kidney disease. Hepatol Int 15:791–803

27. Singh S, Sreenidhi HC, Das P, Devi C (2023) Predicting the Risk of Progression in Indian ADPKD Cohort using PROPKD Score–A Single-Center Retrospective Study. Indian J Nephrol 33:195–201

28. Kataoka H, Fukuoka H, Makabe S, et al (2020) Prediction of renal prognosis in patients with autosomal dominant polycystic kidney disease using PKD1/PKD2 mutations. J Clin Med 9:146

29. Weston BS, Malhas AN, Price RG (2003) Structure–function relationships of the extracellular domain of the autosomal dominant polycystic kidney disease-associated protein, polycystin-1. FEBS Lett 538:8–13

30. Tominaga T, Dutta RK, Joladarashi D, et al (2016) Transcriptional and translational modulation of myo-inositol oxygenase (Miox) by fatty acids: implications in renal tubular injury induced in obesity and diabetes. J Biol Chem 291:1348–1367

31. Tominaga T, Sharma I, Fujita Y, et al (2019) Myo-inositol oxygenase accentuates renal tubular injury initiated by endoplasmic reticulum stress. Am J Physiol Physiol 316:F301–F315

32. Sharma I, Deng F, Liao Y, Kanwar YS (2020) Myo-inositol oxygenase (MIOX) overexpression drives the progression of renal tubulointerstitial injury in diabetes. Diabetes 69:1248–1263

33. Liu W, Xiang J, Wu X, et al (2022) Transcriptome Profiles Reveal a 12-Signature Metabolic Prediction Model and a Novel Role of Myo-Inositol Oxygenase in the Progression of Prostate Cancer. Front Oncol 12:

34. Song X, Di Giovanni V, He N, et al (2009) Systems biology of autosomal dominant polycystic kidney disease (ADPKD): computational identification of gene expression pathways and integrated regulatory networks. Hum Mol Genet 18:2328–2343

35. Kinoshita M, Higashihara E, Kawano H, et al (2016) Technical evaluation: identification of pathogenic mutations in PKD1 and PKD2 in patients with autosomal dominant polycystic kidney disease by next-generation sequencing and use of a comprehensive new classification system. PLoS One 11:e0166288

36. Rossetti S, Consugar MB, Chapman AB, et al (2007) Comprehensive molecular diagnostics in autosomal dominant polycystic kidney disease. J Am Soc Nephrol 18:2143–2160

Table 1: Clinical Features of Autosomal Dominant Polycystic Kidney Disease Patients

Sample ID*	Sex	Age at Sampling/ Diagnosis	Family History	Unilateral/ Bilateral	Size Right Kidney (cm)	Size Left Kidney (cm)	Cyst in other Organ	First Sign	Sign and Symptoms
1_CD1	F	Mid 40s/Mid 40s	Yes	B/L	15.0 x 8.4	15.1 x 8.0	-	NA	NA
2_CD3	M	Mid 50s/early 50s	No	B/L	17.8 x 7.8	18.0 x 8.22	Liver	NA	Generalized body weakness
3_CD8	M	Early 20s/late teenage	Yes	B/L	11.83	10.87	No	NA	Mild Flank Pain
4_CD25	F	Mid 50s/ Early 40s	Yes	B/L	18.1 x 10.2	16.1 x 9.1	-	NA	Fatigue, rare flank pain and weakness, fever
5_CD42	F	Early 30s/Late 20s	Yes	B/L	Normal	Normal	No	Frequent Urination	Weakness, fatigue, fever,Nausea, Dysguesia
6_CD66	F	Early 50s/Early50s	Yes	B/L	19.4 x 10.8	15.5x 9.8	No	Blood in urine	Weakness, fatigue, Nausea, h/o Heamaturia
7_CD73	M	Early 30s/ Late teenage	Yes	B/L	15.9 x 3.68	16.6 x 3.74	No	Flank pain	h/o Heamaturia, mildly bulky pancrease showing STEMT is insitu, bilateral renal parenchyma disease
8_CD78	F	Early 20s/ Late teenage	Yes	B/L	15.2 x 6.1	13.3 x 7.2	Liver, Right Ovary (Simple cysts)	Stomach ache, Stone	Fever, fatigue, headache
9_CD98	M	Late 20s/NA	Yes	B/L	23.1 x 11.6	22.1 x 11.6	No	NA	NA
10_CD103	M	Early 20s/ Late teenage	Younger Sibling with cysts in Rt kidney	U/L Rt Kidney	8.5 x 3.8	8.3 x 3.8	No	General examination	Left flank pain, gas, discomfort while working
11_CD99	M	Late 30s/Early 30s	yes	B/L	Normal	Normal	Liver	NA	Multiple variable and noncommunicating cysts in both kidneys showing haemorrhage; few right concretion (2-3mm), Mid cardiomegaly, diffuse urinary bladder thickning (S/O cystitis); Bulky b/l seminal vesicle; minimal b/l pleural effusion
12_CD24	F	Mid 40s/Mid	First degree	B/L	16.2	16.6	-	NA	Flank pain and swelling, Heamaturiya, eye pain, sometimes fever, dysguisea

		20s	relative with cystic kidneys						sometimes

The table presents the clinical characteristics of ADPKD patients, including information on gender, approximate age at sampling and diagnosis, family history, presence of liver cysts, and symptoms reported by each patient. M: Male, F: Female, Rt: Right, NA: Not available, h/o: history of, B/L: Bilateral, U/L: Unilateral.

* Each sample was assigned a unique study code to ensure confidentiality and anonymity throughout the research process.

Table 2: WES data showing *PKD1* and *PKD2* genetic variants identified in ADPKD patients

Sample ID*	Gene	HGVSP	HGVSC (RsID)	GT	EFFECT	Protein region	Transcript ID	Exon ID	ClinVar	CADDP	Max AF	Max AF Field
1_CD1	*PKD1*	p.Glu2937 Lys	c.8809G>A	HET	MS	REJ Domain Profile region	NM_001009944.3	24	Uncertain Significance	23.3	0	-
	PKD1	p.Thr2710 =	c.8130C>T (rs548582219)	HET	S	REJ Domain Profile region	NM_001009944.3	22	NA	0.005	0.00095007	GNG_AF
2_CD3	*PKD2*	_	c.2358+5G>A (rs1720774022)	HET	ISS		NM_000297.4	12	Uncertain Significance	26.5	0	-
	PKD2	_	c.*174G>T (rs187001642)	HET	UTR 3'		NM_000297.4	15	Uncertain Significance	9.99	0.00179712	1000GP1_AF
3_CD8	*PKD1*	_	c.8017-3C>G	HET	ISS		NM_001009944.3	21	NA	23.4	0	-
4_CD25	*PKD1*	p.Gln149fs *141	c.445delC (rs796052133)	HET	FS	Between LRR1 and WSC domain	NM_001009944.3	4	Pathogenic		0	-
5_CD42	*PKD1*	_	c.8017-3C>G	HET	ISS		NM_001009944.3	21	NA	23.4	0	-
6_CD66	*PKD1*	p.Ser3305f s*84	c.9914_9915del CT (rs1567169638)	HET	FS	Between LH2 and PKD Cation Channel	NM_001009944.3	29	Pathogenic		0	-
7_CD73	*PKD1*	p.His1347f s*83	c.4041_4042del CA (rs2092491511)	HET	FS	PKD 7th Domain	NM_001009944.3	15	Pathogenic		0	-
8_CD78	*PKD1*	p.Ser2792 _Leu2793d el	c.8374_8379del AGCCTG	HET	C Del	REJ Domain Profile region	NM_001009944.3	23	NA		0	-
	PKD1	p.Asp2789 _Pro2790d elinsGlu	c.8367_8369del CCC	HET	CC + C Del	REJ Domain Profile region	NM_001009944.3	23	NA		0	-
	PKD1	p.Leu2776 fs*87	c.8327_8363del TGGCGGGCG AGGAGATCG TGGCCCAGG GCAAGCGCT C	HET	FS	REJ Domain Profile region	NM_001009944.3	23	NA		0	-

9_CD98	*PKD1*	p.Gly2310 Arg	c.6928G>A (rs545933164)	HOM	MS	REJ Domain	NM_001009944.3	16	NA	21	0.00039936	1000GP1_AF
10_CD103	*PKD2*	p.Ser370Asn	c.1109G>A (rs774482918)	HET	MS		NM_000297.4	5	NA	21.9	4.02E-06	GNE_AF
	PKD1	p.Asp2095 Gly	c.6284A>G (rs753250956)	HET	MS	PKD 16th Domain	NM_001009944.3	15	NA	22.8	7.70E-05	GNE_AF
	PKD1	p.Thr938 Met	c.2813C>T (rs74488735)	HET	MS	PKD 3rd Domain	NM_001009944.3	11	NA	0.544	0.03278845	GNE_AF
11_CD99	*PKD1*	p.Glu593*	c.1777G>T	HET	N	Between Lectin C type Domain and PKD 2nd Domain	NM_001009944.3	9	NA	37	0	-
12_CD24	*PKD1*	p.Trp967Arg	c.2899T>C	HET	MS	PKD 3rd Domain	NM_001009944.3	12	NA	27.8	0	-

The table presents the genetic variants identified through WES analysis of ADPKD patients. The table includes information such as sample ID code, gene, amino acid change, Human Genome Variation Society (HGVS) notation for protein and DNA changes, genotype (GT), variant effect, exon number, ClinVar status, CADDP score, and maximum Allele Frequency and its source. MS: Missense, S: Synonymous, FS: Frameshift; C Del: Codon Deletion CC + C Del: Codon Change Plus Codon Deletion; N: Nonsense, ISS: Intron Splice site region; GT: genotype; AF allele frequency; NA: Not available.

* Each sample was assigned a unique study code to ensure confidentiality and anonymity throughout the research process.

Table 3: *PKD1* and *PKD2* Variants Analysis

Gene	HGVSP	HGVSC	ACMG Classification	MUT Assessor	SIFT	PolyPhen2	Mutation Taster	DANN	MetaLR	Aggregated Prediction	Splice AI	dbscSNV Ada	dbscSNV RF	Remarks
PKD1	p.Glu2937Lys	c.8809G>A	PM2	Med (2.63)	Benign (Supporting) (0.28)	-	Deleterious (0.99)	Deleterious (1)	Deleterious (low) (0.52)	Uncertain (0.49)	-	-	-	Not Reported in population databases, two submitthers in clinvar, Mutation taster showed Disease Causing and Variant was neither found in ExAC nor 1000G;
PKD1	p.Thr2710=	c.8130C>T	BS1, BP7	-	-	-	-	-	-	-	-	-	-	Reported in Database
PKD2	-	c.2358+5G>A	PP3, PM2	-	-	-	-	-	-	Deleterious (0.8)	Splice-Altering / strong (0.95)	Deleterious (1)	dbscSNV RF	Not Reported in population databases, two submitthers in clinvar, Splice altering
PKD2	-	c.*174G>T	BP7, BS1	-	-	-	-	-	-	-	Benign (0)	-	-	Reported in population databases, one submitther in clinvar,
PKD1	-	c.8017-3C>G	PM3, PM2	-	-	-	-	-	-	Deleterious (0.8)	Splice-Altering / strong (0.95)	eleterious (1)	Deleterious (0.74)	Not Reported in population databases, reported in one publication
PKD1	p.Gln149fs*141	c.445delC	PVS1, PM2, PP5	-	-	-	-	-	-	Benign (0.02)	Benign (0.01)	-	-	Reported in Database
PKD1	-	c.8017-3C>G	PM3, PM2	-	-	-	-	-	-	Deleterious (0.8)	Splice-Altering / strong (0.95)	eleterious (1)	Deleterious (0.74)	Not Reported in population databases, reported in one publication
PKD1	p.Ser3305fs*84	c.9914_9915delCT	PVS1, PM2, PS4, PP5	-	-	-	-	-	-	Benign (0.02)	Benign (0.01)	-	-	Not Reported in population databases, two submitthers in clinvar
PKD1	p.His1347fs*83	c.4041_4042delCA	PVS1, PM2, PS4, PP5	-	-	-	-	-	-	-	-	-	-	Not Reported in population databases, two submitthers in clinvar

PKD1	p.Ser2792_Leu2793del	c.8374_8379delAGCCTG	PM2, PM4	-	-	-	-	-	-	-	-	-	-	Novel, Not Reported in population databases or publication
PKD1	p.Asp2789_Pro2790delinsGlu	c.8367_8369delCCC	PM2, PM4	-	-	-	-	-	-	-	Benign (0.01)		-	Novel, Not Reported in population databases or publication
PKD1	p.Leu2776fs*87	c.8327_8363delTGGCGGGCGAGGAGATCGTGGCCCAGGGCAAGCGCTC	PVS1, PM2	-	-	-	-	-	-	-	-	-	-	Novel, Not Reported in population databases or publication
PKD1	p.Gly2310Arg	c.6928G>A	BS1	Med (1.95)	Benign (Moderate) (0.622)	Uncertain (0.92)	Benign (0)	Deleterious (0.92)	Benign (low) (0.36)	Uncertain (0.53)	-	-	-	Reported in Database
PKD2	p.Ser370Asn	c.1109G>A	PM2, BP4	Lo (1.12)	Benign (Supporting) (0.03)	Benign (Supporting) (0.03)	Deleterious (low) (0.58)	Deleterious (0.98)	Benign (low) (0.21)	Benign (0.14)	-	-	-	Reported in Database
PKD1	p.Asp2095Gly	c.6284A>G	N/A	Hi (4.01)	Uncertain (0.062)	Uncertain (0.97)	Benign (0.01)	Deleterious (1)	Deleterious (low) (0.55)	Uncertain (0.61)	-	-	-	Reported in Database
PKD1	p.Thr938Met	c.2813C>T	N/A	Lo (1.15)	Benign (Supporting) (0.214)	Uncertain (0.15)	Benign (0)	Deleterious (0.96)	Benign (0.03)	Uncertain (0.28)	-	-	-	Reported in Database
PKD1	p.Glu593*	c.1777G>T	PVS1, PM2	-	Deleterious	-	Deleterious (1)	Deleterious (1)	-	-	-	-	-	Not reported in Database. Reported in one publication [28]
PKD1	p.Trp967Arg	c.2899T>C	PP3, PM2	Lo (1.87)	Deleterious	-	Deleterious (1)	Deleterious (1)	Deleterious (0.74)	Deleterious (0.99)	-	-	-	Not Reported in population databases, reported in publication [35, 36]

The table presents the results of WES data analysis for *PKD1* and *PKD2* variants identified in ADPKD patients. The table includes information on the gene affected by the variant, and the details such as the Human Genome Variation Society Protein (HGVSP) and Coding (HGVSC) notations, the American College of Medical Genetics (ACMG) classification, MUT Assessor score, and predictions from various computational tools including SIFT, PolyPhen2, MutationTaster, DANN, MetaLR, and SpliceAI, dbscSNV Ada and dbscSNV RF scores, and remarks or relevant notes regarding the variants identified. – not applicable/available.

Table 4: *PKD1* Exon Number and Protein Amino Acid Intervals

***PKD1* Exon No.**	**Amino Acid (Protein ID: NP_001009944.3)**	***PKD1* Exon No.**	**Amino Acid (Protein ID: NP_001009944.3)**	***PKD1* Exon No.**	**Amino Acid (Protein ID: NP_001009944.3)**
1	01-72	17	2356-2403	33	3407-3469
2	72-96	18	2404-2497	34	3469-3500
3	96-120	19	2497-2568	35	3500-3540
4	120-177	20	2565-2621	36	3540-3607
5	177-401	21	2622-2672	37	3608-3672
6	401-462	22	2673-2721	38	3673-3719
7	462-536	23	2721-2931	39	3719-3757
8	536-574	24	2931-2983	40	3757-3804
9	574-617	25	2983-3067	41	3804-3846
10	617-699	26	3067-3133	42	3847-3904
11	700-951	27	3133-3190	43	3905-4001
12	952-995	28	3190-3238	44	4002-4046
13	996-1054	29	3238-3308	45	4047-4148
14	1054-1099	30	3308-3350	46	4149-4303
15	1099-2305	31	3351-3389		
16	2306-2355	32	3390-3407		
Note: The same amino acid number in the interval is shared by both the exons					

The table provides the exon numbers and corresponding protein amino acid intervals for the *PKD1* gene, facilitating the identification and characterization of genetic variants associated with ADPKD.

Table 5: PKD1 Amino Acid Positions and corresponding Motifs or Domains

PKD1 AA position	PKD1 Motif or Domain
16-21	MYRISTYL; N-myristoylation site
29-34	MYRISTYL; N-myristoylation site
32-66	LRRNT; Leucine rich repeat N-terminal domain
32-66	LRRNT; Leucine rich repeat N-terminal domain
52-54	PKC_PHOSPHO_SITE;Protein kinase C phosphorylation site
52-122	LRR_SDS22; SDS22+-like LRR profile/LRR_TP; Treponema pallidum (Tp) LRR profile/LRR_TYPICAL; Typical LRR profile
70-73	CK2_PHOSPHO_SITE; Casein kinase II phosphorylation site
72-93	LEUCINE_ZIPPER; Leucine zipper pattern
85-90	MYRISTYL; N-myristoylation site
92-114	LRR_1; Leucine Rich Repeat
104-107	CK2_PHOSPHO_SITE; Casein kinase II phosphorylation site
109-114	MYRISTYL; N-myristoylation site
152-177	LRRCT; Leucine rich repeat C-terminal domain
159-164	MYRISTYL; N-myristoylation site
177-271	WSC; WSC domain profile
180-261	WSC; WSC domain
190-195	MYRISTYL; N-myristoylation site
218-223	MYRISTYL; N-myristoylation site
251-283	PRO_RICH; roline-rich region profile
258-260	PKC_PHOSPHO_SITE;Protein kinase C phosphorylation site
277-352	PKD; PKD domain
287-292	MYRISTYL; N-myristoylation site
299-359	PKD; Polycystic kidney disease (PKD) domain profile
303-306	CK2_PHOSPHO_SITE; Casein kinase II phosphorylation site
322-324	PKC_PHOSPHO_SITE;Protein kinase C phosphorylation site
340-345	MYRISTYL; N-myristoylation site
383-386	CK2_PHOSPHO_SITE; Casein kinase II phosphorylation site
384-389	MYRISTYL; N-myristoylation site
408-411	CK2_PHOSPHO_SITE; Casein kinase II phosphorylation site
415-420	MYRISTYL; N-myristoylation site
415-531	C_TYPE_LECTIN_2; C-type lectin domain profile
425-532	Lectin_C; Lectin C-type domain
441-446	MYRISTYL; N-myristoylation site
547-552	MYRISTYL; N-myristoylation site
580-585	MYRISTYL; N-myristoylation site
590-593	CK2_PHOSPHO_SITE; Casein kinase II phosphorylation site

617-622	MYRISTYL; N-myristoylation site
623-626	CK2_PHOSPHO_SITE; Casein kinase II phosphorylation site
649-654	MYRISTYL; N-myristoylation site
677-682	MYRISTYL; N-myristoylation site
803-808	MYRISTYL; N-myristoylation site
852-857	MYRISTYL; N-myristoylation site
855-928	PKD; PKD domain
858-860	PKC_PHOSPHO_SITE;Protein kinase C phosphorylation site
863-868	MYRISTYL; N-myristoylation site
867-869	PKC_PHOSPHO_SITE;Protein kinase C phosphorylation site
903-906	CK2_PHOSPHO_SITE; Casein kinase II phosphorylation site
923-925	PKC_PHOSPHO_SITE;Protein kinase C phosphorylation site
927-930	CK2_PHOSPHO_SITE; Casein kinase II phosphorylation site
937-1013	PKD; PKD domain
958-1020	PKD; Polycystic kidney disease (PKD) domain profile
968-971	CK2_PHOSPHO_SITE; Casein kinase II phosphorylation site
1021-1026	MYRISTYL; N-myristoylation site
1024-1122	PKD; PKD domain
1047-1050	CK2_PHOSPHO_SITE; Casein kinase II phosphorylation site
1050-1129	PKD; Polycystic kidney disease (PKD) domain profile
1056-1059	CK2_PHOSPHO_SITE; Casein kinase II phosphorylation site
1074-1094	EspF; EspF protein repeat
1121-1123	PKC_PHOSPHO_SITE;Protein kinase C phosphorylation site
1127-1215	PKD; Polycystic kidney disease (PKD) domain profile
1131-1208	PKD; PKD domain
1132-1137	MYRISTYL; N-myristoylation site
1156-1161	MYRISTYL; N-myristoylation site
1217-1291	PKD; PKD domain
1236-1293	PKD; Polycystic kidney disease (PKD) domain profile
1250-1255	MYRISTYL; N-myristoylation site
1254-1257	CK2_PHOSPHO_SITE; Casein kinase II phosphorylation site
1301-1376	PKD; PKD domain
1307-1310	CK2_PHOSPHO_SITE; Casein kinase II phosphorylation site
1318-1383	PKD; Polycystic kidney disease (PKD) domain profile
1329-1332	CK2_PHOSPHO_SITE; Casein kinase II phosphorylation site
1333-1338	MYRISTYL; N-myristoylation site
1338-1340	PKC_PHOSPHO_SITE;Protein kinase C phosphorylation site
1362-1364	PKC_PHOSPHO_SITE;Protein kinase C phosphorylation site
1385-1462	PKD; PKD domain
1409-1469	PKD; Polycystic kidney disease (PKD) domain profile
1417-1422	MYRISTYL; N-myristoylation site
1470-1472	PKC_PHOSPHO_SITE;Protein kinase C phosphorylation site

1471-1544	PKD; PKD domain
1487-1551	PKD; Polycystic kidney disease (PKD) domain profile
1519-1522	CK2_PHOSPHO_SITE; Casein kinase II phosphorylation site
1524-1526	PKC_PHOSPHO_SITE;Protein kinase C phosphorylation site
1534-1537	CK2_PHOSPHO_SITE; Casein kinase II phosphorylation site
1543-1545	PKC_PHOSPHO_SITE;Protein kinase C phosphorylation site
1550-1555	MYRISTYL; N-myristoylation site
1553-1628	PKD; PKD domain
1554-1557	ASN_GLYCOSYLATION; N-glycosylation site
1570-1573	CK2_PHOSPHO_SITE; Casein kinase II phosphorylation site
1573-1635	PKD; Polycystic kidney disease (PKD) domain profile
1600-1602	PKC_PHOSPHO_SITE;Protein kinase C phosphorylation site
1619-1622	CK2_PHOSPHO_SITE; Casein kinase II phosphorylation site
1637-1714	PKD; PKD domain
1659-1664	MYRISTYL; N-myristoylation site
1659-1706	PKD; Polycystic kidney disease (PKD) domain profile
1678-1683	MYRISTYL; N-myristoylation site
1679-1681	PKC_PHOSPHO_SITE;Protein kinase C phosphorylation site
1686-1689	CK2_PHOSPHO_SITE; Casein kinase II phosphorylation site
1704-1709	MYRISTYL; N-myristoylation site
1719-1805	PKD; Polycystic kidney disease (PKD) domain profile
1723-1798	PKD; PKD domain
1747-1752	MYRISTYL; N-myristoylation site
1753-1756	CK2_PHOSPHO_SITE; Casein kinase II phosphorylation site
1784-1789	MYRISTYL; N-myristoylation site
1806-1808	PKC_PHOSPHO_SITE;Protein kinase C phosphorylation site
1807-1883	PKD; PKD domain
1814-1819	MYRISTYL; N-myristoylation site
1827-1832	MYRISTYL; N-myristoylation site
1831-1890	PKD; Polycystic kidney disease (PKD) domain profile
1845-1847	PKC_PHOSPHO_SITE;Protein kinase C phosphorylation site
1863-1865	PKC_PHOSPHO_SITE;Protein kinase C phosphorylation site
1882-1885	CK2_PHOSPHO_SITE; Casein kinase II phosphorylation site
1892-1967	PKD; PKD domain
1895-1897	PKC_PHOSPHO_SITE;Protein kinase C phosphorylation site
1913-1974	PKD; Polycystic kidney disease (PKD) domain profile
1914-1919	MYRISTYL; N-myristoylation site
1918-1920	PKC_PHOSPHO_SITE;Protein kinase C phosphorylation site
1949-1951	PKC_PHOSPHO_SITE;Protein kinase C phosphorylation site
1976-2057	PKD; PKD domain
1983-1988	MYRISTYL; N-myristoylation site

1986-1989	CK2_PHOSPHO_SITE; Casein kinase II phosphorylation site
1988-1990	PKC_PHOSPHO_SITE;Protein kinase C phosphorylation site
1993-1995	PKC_PHOSPHO_SITE;Protein kinase C phosphorylation site
1999-2004	MYRISTYL; N-myristoylation site
2022-2025	CK2_PHOSPHO_SITE; Casein kinase II phosphorylation site
2022-2024	PKC_PHOSPHO_SITE;Protein kinase C phosphorylation site
2066-2141	PKD; PKD domain
2073-2075	PKC_PHOSPHO_SITE;Protein kinase C phosphorylation site
2074-2148	PKD; Polycystic kidney disease (PKD) domain profile
2075-2087	PSGP;Apopolysialoglycoprotein (PSGP)
2086-2088	PKC_PHOSPHO_SITE;Protein kinase C phosphorylation site
2146-2833	REJ; REJ domain profile
2164-2166	PKC_PHOSPHO_SITE;Protein kinase C phosphorylation site
2168-2693	REJ; REJ domain
2208-2213	MYRISTYL; N-myristoylation site
2235-2238	CK2_PHOSPHO_SITE; Casein kinase II phosphorylation site
2264-2266	PKC_PHOSPHO_SITE;Protein kinase C phosphorylation site
2304-2307	CK2_PHOSPHO_SITE; Casein kinase II phosphorylation site
2304-2306	PKC_PHOSPHO_SITE;Protein kinase C phosphorylation site
2310-2315	MYRISTYL; N-myristoylation site
2333-2338	MYRISTYL; N-myristoylation site
2345-2348	Amidation site
2352-2362	FARP; FMRFamide related peptide family
2360-2362	PKC_PHOSPHO_SITE;Protein kinase C phosphorylation site
2372-2374	PKC_PHOSPHO_SITE;Protein kinase C phosphorylation site
2399-2404	MYRISTYL; N-myristoylation site
2400-2402	PKC_PHOSPHO_SITE;Protein kinase C phosphorylation site
2411-2413	PKC_PHOSPHO_SITE;Protein kinase C phosphorylation site
2454-2457	CK2_PHOSPHO_SITE; Casein kinase II phosphorylation site
2462-2464	PKC_PHOSPHO_SITE;Protein kinase C phosphorylation site
2475-2477	PKC_PHOSPHO_SITE;Protein kinase C phosphorylation site
2482-2487	MYRISTYL; N-myristoylation site
2488-2490	PKC_PHOSPHO_SITE;Protein kinase C phosphorylation site
2530-2535	MYRISTYL; N-myristoylation site
2573-2576	CK2_PHOSPHO_SITE; Casein kinase II phosphorylation site
2579-2584	MYRISTYL; N-myristoylation site
2590-2595	MYRISTYL; N-myristoylation site
2652-2654	PKC_PHOSPHO_SITE;Protein kinase C phosphorylation site
2657-2660	CK2_PHOSPHO_SITE; Casein kinase II phosphorylation site
2784-2787	Amidation site
2803-2808	MYRISTYL; N-myristoylation site

2807-2810	CK2_PHOSPHO_SITE; Casein kinase II phosphorylation site
2814-2819	MYRISTYL; N-myristoylation site
2845-2847	PKC_PHOSPHO_SITE;Protein kinase C phosphorylation site
2868-2870	PKC_PHOSPHO_SITE;Protein kinase C phosphorylation site
2873-2875	PKC_PHOSPHO_SITE;Protein kinase C phosphorylation site
2906-2911	MYRISTYL; N-myristoylation site
2927-2930	CK2_PHOSPHO_SITE; Casein kinase II phosphorylation site
2960-2962	PKC_PHOSPHO_SITE;Protein kinase C phosphorylation site
3009-3014	MYRISTYL; N-myristoylation site
3011-3055	GPS; Latrophilin/CL-1-like GPS domain
3011-3055	GPS; Latrophilin/CL-1-like GPS domain
3012-3061	GPS; GPS domain profile
3019-3022	CK2_PHOSPHO_SITE; Casein kinase II phosphorylation site
3037-3039	PKC_PHOSPHO_SITE;Protein kinase C phosphorylation site
3118-3233	PLAT; PLAT/LH2 domain
3131-3136	MYRISTYL; N-myristoylation site
3190-3195	MYRISTYL; N-myristoylation site
3207-3209	PKC_PHOSPHO_SITE;Protein kinase C phosphorylation site
3265-3268	CK2_PHOSPHO_SITE; Casein kinase II phosphorylation site
3326-3331	MYRISTYL; N-myristoylation site
3369-3372	CK2_PHOSPHO_SITE; Casein kinase II phosphorylation site
3374-3377	CK2_PHOSPHO_SITE; Casein kinase II phosphorylation site
3394-3399	MYRISTYL; N-myristoylation site
3419-3422	CK2_PHOSPHO_SITE; Casein kinase II phosphorylation site
3466-3469	CK2_PHOSPHO_SITE; Casein kinase II phosphorylation site
3490-3493	CK2_PHOSPHO_SITE; Casein kinase II phosphorylation site
3503-3506	CK2_PHOSPHO_SITE; Casein kinase II phosphorylation site
3540-3545	MYRISTYL; N-myristoylation site
3583-3588	MYRISTYL; N-myristoylation site
3607-3614	TYR_PHOSPHO_SITE;Tyrosine kinase phosphorylation site
3621-3629	LSPR; Coagulation Factor V LSPD Repeat
3629-3632	CK2_PHOSPHO_SITE; Casein kinase II phosphorylation site
3640-3642	PKC_PHOSPHO_SITE;Protein kinase C phosphorylation site
3669-3674	MYRISTYL; N-myristoylation site
3688-3691	CK2_PHOSPHO_SITE; Casein kinase II phosphorylation site
3711-4113	PKD_channel; Polycystin cation channel
3718-3721	CK2_PHOSPHO_SITE; Casein kinase II phosphorylation site
3740-3743	CK2_PHOSPHO_SITE; Casein kinase II phosphorylation site
3753-3759	TYR_PHOSPHO_SITE;Tyrosine kinase phosphorylation site
3774-3779	MYRISTYL; N-myristoylation site
3777-3780	CK2_PHOSPHO_SITE; Casein kinase II phosphorylation site

3798-3801	CK2_PHOSPHO_SITE; Casein kinase II phosphorylation site
3826-3829	CK2_PHOSPHO_SITE; Casein kinase II phosphorylation site
3862-3867	MYRISTYL; N-myristoylation site
3868-3870	PKC_PHOSPHO_SITE;Protein kinase C phosphorylation site
3884-3886	PKC_PHOSPHO_SITE;Protein kinase C phosphorylation site
3891-3894	CAMP_PHOSPHO_SITE; cAMP- and cGMP-dependent protein kinase phosphorylation site
3972-3975	CAMP_PHOSPHO_SITE; cAMP- and cGMP-dependent protein kinase phosphorylation site
3975-3978	CK2_PHOSPHO_SITE; Casein kinase II phosphorylation site
3989-3994	MYRISTYL; N-myristoylation site
3990-4101	LEU_RICH; Leucine-rich region profile
4028-4033	MYRISTYL; N-myristoylation site
4037-4042	MYRISTYL; N-myristoylation site
4050-4053	CK2_PHOSPHO_SITE; Casein kinase II phosphorylation site
4068-4073	MYRISTYL; N-myristoylation site
4119-4127	TYR_PHOSPHO_SITE;Tyrosine kinase phosphorylation site
4163-4200	SER_RICH; Serine-rich region profile
4165-4167	PKC_PHOSPHO_SITE;Protein kinase C phosphorylation site
4181-4186	MYRISTYL; N-myristoylation site
4192-4195	CK2_PHOSPHO_SITE; Casein kinase II phosphorylation site
4196-4201	MYRISTYL; N-myristoylation site
4206-4209	CK2_PHOSPHO_SITE; Casein kinase II phosphorylation site
4224-4227	CK2_PHOSPHO_SITE; Casein kinase II phosphorylation site
4247-4250	Amidation site
4249-4252	CAMP_PHOSPHO_SITE; cAMP- and cGMP-dependent protein kinase phosphorylation site
4251-4253	PKC_PHOSPHO_SITE;Protein kinase C phosphorylation site
4258-4260	PKC_PHOSPHO_SITE;Protein kinase C phosphorylation site
4259-4278	OGFr_III; Opioid growth factor receptor repeat
4265-4270	MYRISTYL; N-myristoylation site
4280-4285	MYRISTYL; N-myristoylation site

The table presents a comparison between the amino acid positions in the PKD1 protein and the motifs or domains identified by Motif Scan analysis. The first column lists the amino acid positions in PKD1, while the second column indicates the motifs or domains identified by Motif Scan. The motifs correspond to specific protein domains or functional regions within the PKD1 protein. This provides insights into the potential functional significance of genetic variants affecting amino acid residues in PKD1 and their association with known protein parts.

Table 6: Conserved Domains of PKD1 Protein

Name	Accession	Amino acid Interval	E-value
PCC super family (polycystin cation channel protein)	cl28216	97-2728	0.00E+00
PKD channel super family (Polycystin cation channel)	cl37568	3713-4113	2.37E-106
PLAT polycystin (PLAT/LH2 domain of polycystin-1 like proteins)	cd01752	3118-3237	8.86E-58
GPS super family (GPCR proteolysis site, GPS, motif)	cl02559	3011-3060	3.08E-10
PPP1R42 super family (protein phosphatase 1 regulatory subunit 42)	cl42388	54-127	6.08E-09

The table represents the conserved domains identified within the PKD1 protein using the NCBI Conserved Domains Database. Each domain is listed along with its corresponding accession number. These conserved domains provide information of the structural and functional characteristics of the PKD1 protein**.**

Table 7: PC1 Domains and Anticipated Function

PC1 Domain	Anticipated Function
Leucine-rich repeat (LRR) domains	Signal transduction pathways and PC1's involvement in cell-cell and cell-matrix interactions
WSC (cell wall integrity and stress response components)	Stress-activated pathways regulator
C-type lectin domain	The C-type lectin domain binds a diverse array of carbohydrate ligands, suggesting its involvement in protein-protein interactions, potentially contributing to cell adhesion and signaling processes
Low-density lipoprotein-A domain (LDL-A)	Cysteine-rich and hydrophobic in nature
PKD repeats	Vital mediators of cell-cell interactions and normal renal development
REJ domain	Acts as a regulator of ion transport, potentially facilitating PC1 functions and supporting calcium influx
GPS motif	Sites of proteolytic cleavage potentially crucial for signal transduction through PC-1
PLAT domain (Polycystin-1, Lipoxygenase, Alpha-Toxin)	Protein-protein and protein-lipid binding involved in cell signaling pathways
11 transmembrane domains	Likely serve as channels or pores for the transport of ions or other molecules across cell membranes facilitating various cellular processes such as signal transduction, ion homeostasis
C-terminal tail (189aa) including a 74aa G-protein binding domain (GBD) followed by α-helical coiled coil domain (amino acids 4214–4248)	Regulates downstream signaling pathways, undergoes proteolytic cleavage. GBD regulates heterotrimeric G protein signaling through direct interactions with G protein subunits.

The table summarizes the domains of PC1 and their anticipated functions based on existing literature and studies. Each domain plays a crucial role in mediating various cellular interactions and signaling pathways, contributing to the overall function of PC1 in maintaining cellular homeostasis and regulating key physiological processes.

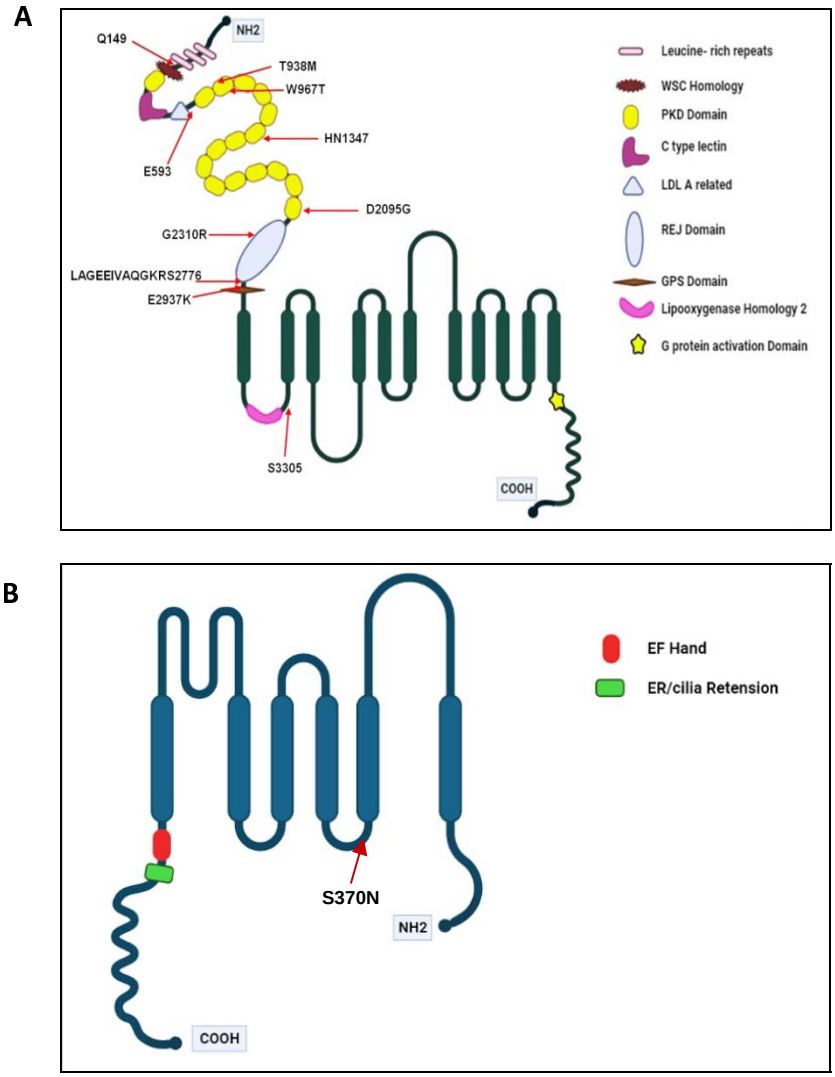

Figure 1: Schematic representation of the coding region variants' location in protein structure of PKD1 and PKD2. A) PKD1/PC1 is a large transmembrane protein with multiple domains, including N-terminal region (NH_2), leucine-rich repeat (LRR) domain, cell wall integrity and stress component (WSC) domain, C-type lectin domain, low density lipoprotein-A (LDL-A) domain, Ig-like 16 PKD repeats, receptor for egg jelly (REJ), GPCR proteolytic site (GPS) comprising N-terminal region followed by PLAT (Polycystin-1, Lipoxygenase, Alpha-Toxin) domain, 11 transmembrane domains, G protein activation domain and C-terminal coiled-coil tail. B) PKD2/PC2 is a smaller protein with six transmembrane domains (TM1-TM6) and cytoplasmic N- and C-termini. Both proteins are essential components of the polycystin complex involved in calcium signaling and regulation of renal tubular cell proliferation and differentiation.

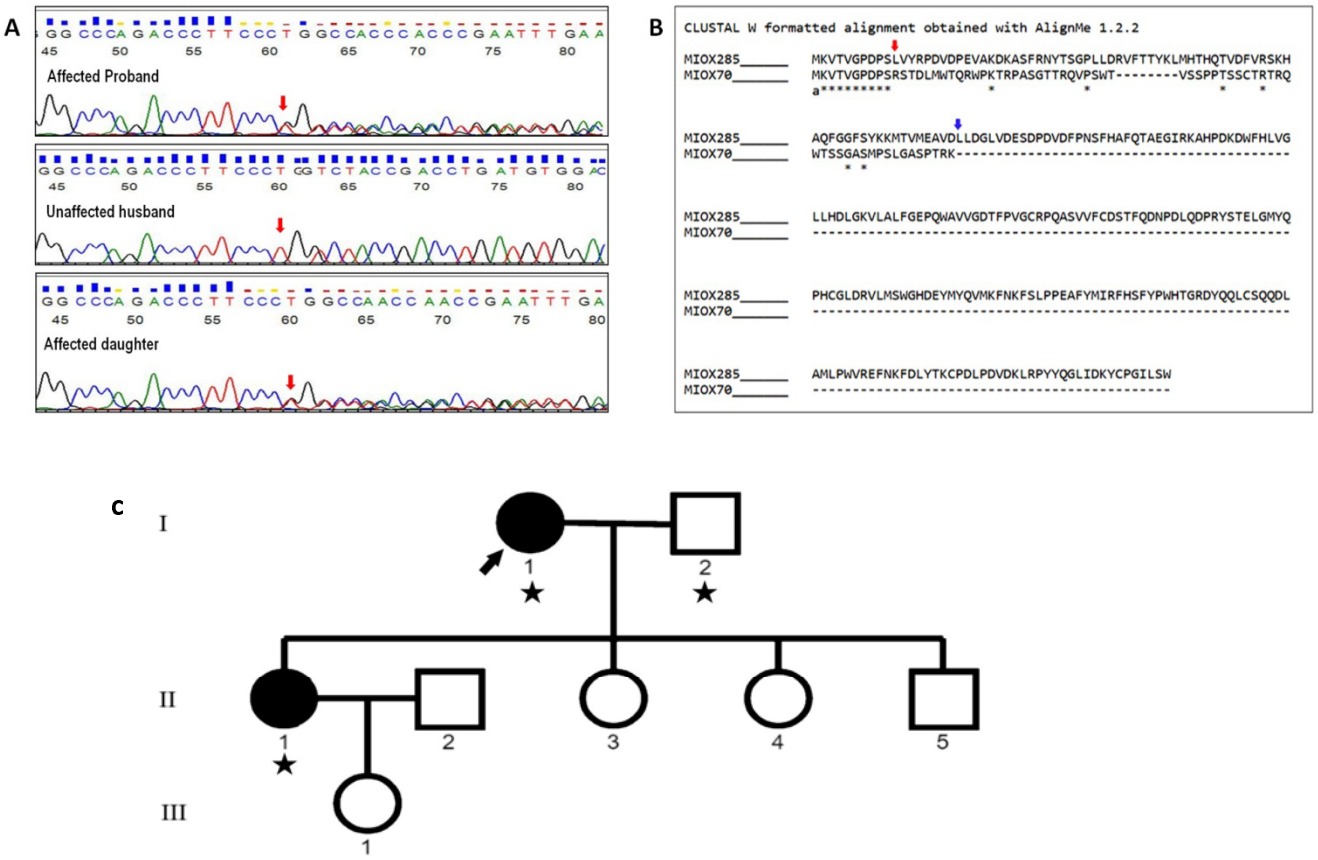

Figure 2: Sanger sequencing confirmation and alignment of normal (Miox285) and mutated (Miox70) protein sequence. A) Sanger sequencing confirmed the heterozygous deletion variant in the proband and affected daughter. Red arrow points the variant base. B) The alignment of normal (Miox285) and mutated (Miox70) protein sequence The Asterisks (*) represents the matched amino acids. Red and blue arrows indicate the amino acid change due to nucleotide change and truncation position respectively. Frame-shift deletion leads to truncated protein of 70 amino acids as compared to wild protein of 285 amino acids. C) Pedigree of the ADPKD subject. Star (★) indicates the trio undergone WES.

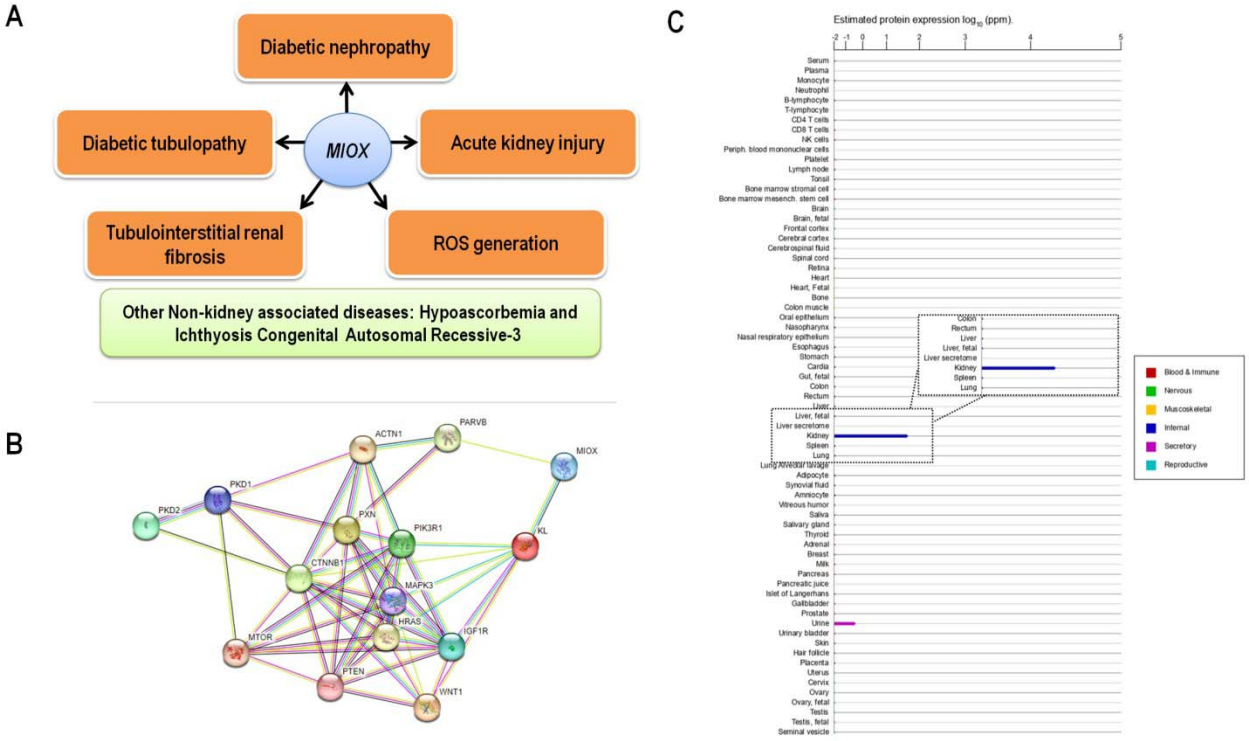

Figure 3: Role of MIOX protein. A) Association of *MIOX* in kidney and non-kidney diseases. B) Representative image depicting different types of interactions among common genes in *PKD1* and *MIOX* STRING interaction networks. C) Integrated Proteomics: protein expression in normal tissues and cell lines from Proteomics DB and MOPED for *MIOX*.

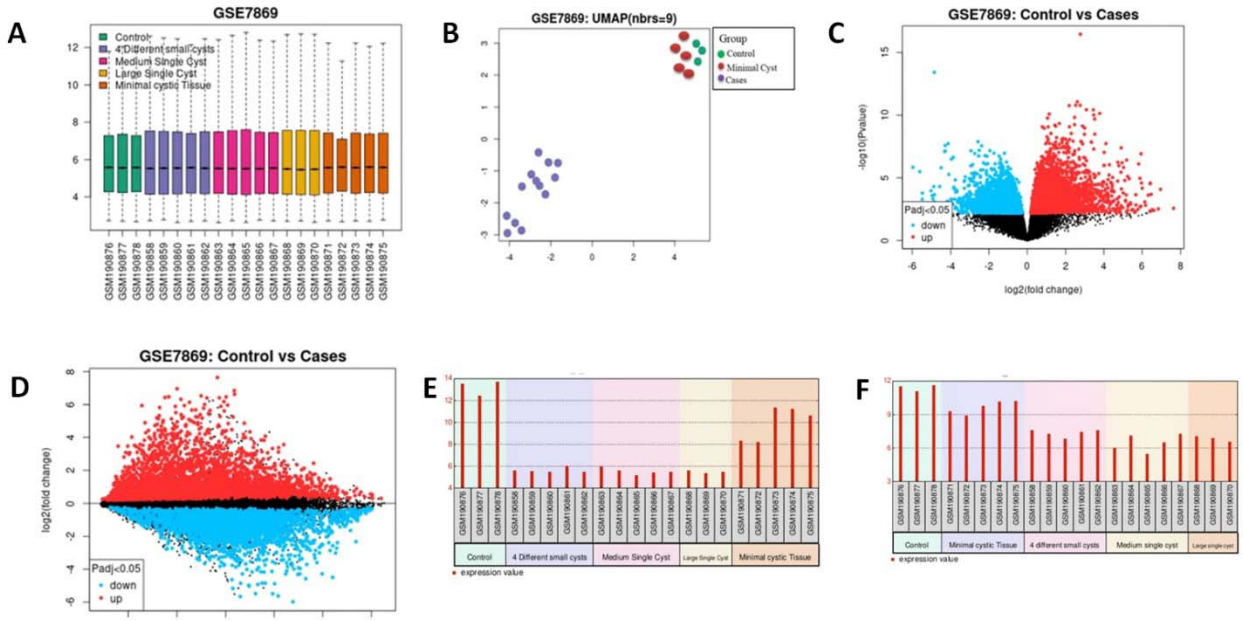

Figure 4: *MIOX* differential expression study in PKD1 cysts. A) Samples are colored based on groupings. Median-centered values indicate that the data are cross-comparable and normalized. B) The dimension reduction method known as uniform manifold approximation and projection (UMAP) representing the relationships between different cyst samples. C & D) The differentially expressed genes are depicted by volcano and mean difference plot. The red and sky-blue dots reflect up regulated and down regulated genes respectively. E) Expression of *MIOX* in cystic samples of ADPKD patients is down regulated as compared to minimal cystic tissues and control tissue samples. F) *KL* gene expression is down regulated as compared to minimal cystic tissues and control tissue samples.